CRYSTAL GROWTH & DESIGN

ARTICLE

pubs.acs.org/crystal

Investigations into the Impact of the Template Layer on ZnO Nanowire Arrays Made Using Low Temperature Wet Chemical Growth

Róbert Erdélyi,[†,‡] Takahiro Nagata,[§] David J. Rogers,[∥,⊥] Ferechteh H. Teherani,[∥] Zsolt E. Horváth,[†] Zoltán Lábadi,[†] Zsófia Baji,[†] Yutaka Wakayama,[§] and János Volk*[,†]

[†]Research Institute for Technical Physics and Materials Science, 1121 Budapest, Konkoly Thege M. út 29-33, Hungary

[‡]University of Pannonia, Faculty of Information Technology, 8200 Veszprém, Egyetem u. 10, Hungary

[§]Advanced Electric Materials Center, National Institute for Materials Science, 1-1 Namiki, Tsukuba, Ibaraki 305-0044, Japan

[∥]Nanovation SARL, 103 bis Rue de Versailles, Orsay 91400, France

[⊥]SUPA, School of Physics and Astronomy, University of St. Andrews, St. Andrews KY16 9SS, U.K.

ABSTRACT: The impact of various ZnO templates on the alignment and geometry of wet-chemically grown vertical ZnO nanowire (NW) arrays was investigated. The NWs were seeded at nucleation windows which were patterned in poly(methyl methacrylate)-coated ZnO surfaces using electron beam lithography. This growth approach was shown to have the potential for low-cost and low-temperature fabrication of regular, highly aligned, and transparent NW arrays with tunable conductivities on cheap substrates with precise engineering of the NW dimensions and positioning. The compared ZnO templates included a single crystal ZnO substrate, an epitaxial film on a c-sapphire substrate, and polycrystalline films on Si(111), Si-(100), and Pt/c-sapphire. Scanning electron microscopy and X-ray diffraction revealed that the alignment, crystal structure, and geometry of the NW arrays were dictated by the crystal structure of the underlying ZnO, while the influence of the surface roughness was negligible. Thus, the choice of seed layer crystallinity gives control over the NW form, alignment, and in-plane crystallographic orientation. In particular, hydrothermal ZnO substrates and epitaxial ZnO layers grown on c-sapphire by pulsed laser deposition gave similar NW arrays with very regular form, strong vertical alignment, and a common relative orientation of their hexagonal crystal facets in the surface plane.

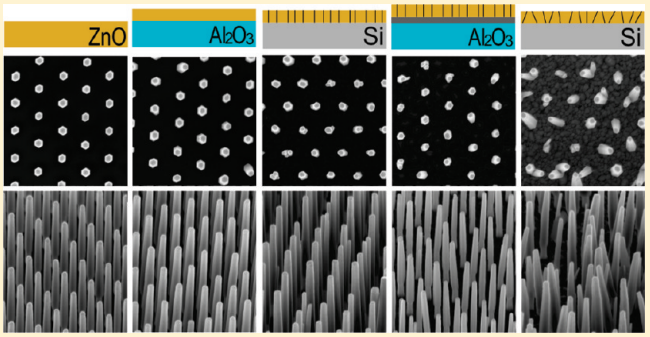

INTRODUCTION

Vertically aligned ZnO nanowire (NW) and nanorod (NR) arrays are currently attracting a great deal of interest due to a variety of potential applications, ranging from photovoltaics, light emitting devices,[1] and piezotronics through to chemical, biological, and gas sensing.[2] As well as their diverse needs in terms of functionalization and device structure, each of these applications has different requirements in terms of nanostructure geometry, spacing, and alignment. For example, Xu et al. reported that arrays of NW near UV/blue light emitting diodes showed enhanced electroluminescence when there was better vertical alignment and length uniformity.[3] The same was found to apply for NW "nanogenerator" arrays, in which more highly ordered, more vertically oriented ZnO NWs/NRs gave improved performance.[4,5] High aspect ratio is found to be important for ZnO NWs used as electrodes in dye-sensitized solar cells.[6,7] Near-surface light wave manipulation by means of an inverse designed homoepitaxial ZnO NR array[8] and rod type photonic crystal optical line defect waveguides[9] both require very good alignment and precise control of NW/NR dimensions. Wang et al., on the other hand, reported that ZnO NW gas sensors showed excellent response for H_2, NH_3, and CO detection irrespective of the degree of alignment.[10]

In previous work, it was demonstrated that regular epitaxial arrays of highly uniform ZnO NRs could be formed homoepitaxially on ZnO single crystals by hydrothermal growth.[11] However, for most applications, an alternative substrate material would be preferable to (i) reduce the cost, (ii) integrate the nanostructure with conventional substrates, e.g. Si, sapphire, or glass, and (iii) attain light confinement in the NR/NW by refractive index contrast at the bottom of the cavity. Heteroepitaxial ZnO NWs can be grown on lattice-matched substrates by several dry deposition methods.[12−14] However, in the case of wet chemical methods, a ZnO seed layer template is required. This seed layer has been found to strongly influence the geometry and orientation of the NRs/NWs which are grown on top.[15] In this work, the effect of the seed layer on the geometry and alignment of patterned vertical ZnO NWs is investigated

Received: March 4, 2011
Revised: April 13, 2011
Published: April 15, 2011

dx.doi.org/10.1021/cg2002755 | *Cryst. Growth Des.* 2011, 11, 2515–2519

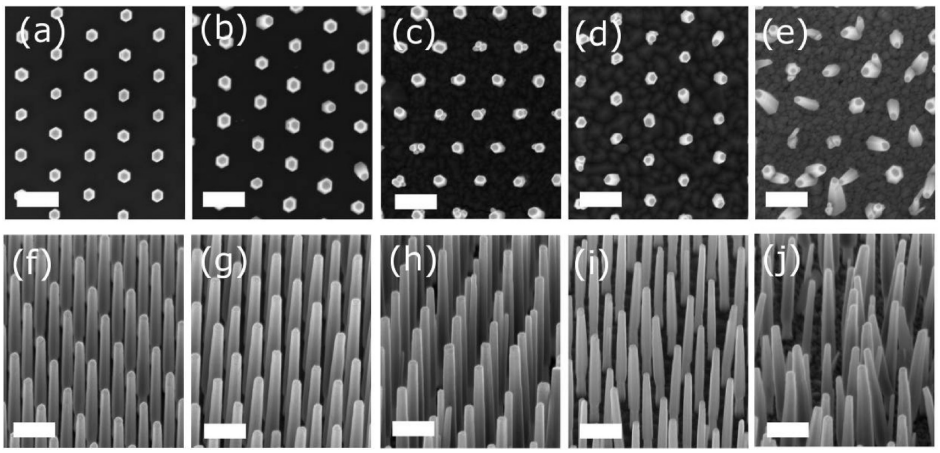

Figure 1. Top- (upper row) and tilted-view (lower row) scanning electron micrographs of vertical ZnO nanowires grown on different substrates (the length of the white scale bar is 500 nm): ZnO single crystal (a and f); PLD deposited ZnO on c-Al_2O_3 (0001) (b and g); PLD deposited ZnO on Si(111) (c and h); PLD deposited ZnO on Pt/c-Al_2O_3(0001) (d and i); reactive magnetron sputtered ZnO on Si(100) (e and j).

through a comparative study of five different types of ZnO seed surfaces. Although patterned growth of ZnO NWs/NRs has already been proposed by several groups on different ZnO seed layers, such as sputtered,[16,17] MOCVD,[18] colloidal,[15] or hydrothermally grown textured[19] thin films, it was not possible to obtain as regular and uniform arrays as those grown on ZnO single crystals.[8,11] This report examines the impact of seed layer with the aim of understanding the factors which influenced the regularity and uniformity of the NW arrays.

EXPERIMENTAL SECTION

The first of the five seed layers was the Zn terminated surface of a *c*-axis oriented, hydrothermal ZnO single crystal (CrysTec GmbH; denoted as "BULK"). The second ZnO seed layer was an epitaxial ZnO thin film grown by pulsed laser deposition (PLD) on c-sapphire (denoted as "PLD/sapphire") using a KrF excimer laser (248 nm).[20] The third ZnO seed layer was ZnO grown by PLD Si(111) (denoted as "PLD/Si").[21] The fourth ZnO seed layer was also deposited by PLD onto c-sapphire, but this time a 100 nm thick highly textured (111) oriented Pt buffer layer was deposited prior to the ZnO growth in a DC magnetron sputtering system, as described elsewhere.[22] This sample was denoted as "PLD/Pt/sapphire". The fifth seed layer was grown on a Si(100) wafer in Ar/O_2 atmosphere by DC reactive magnetron sputtering of an Al doped (2 wt %) Zn target (denoted as "Sputt/Si"). In order to stabilize the glow discharge, a pulse signal was added to the direct current voltage. The deposition was carried out without bias voltage or substrate preheating.[23] It should be noted that no attempt was made to remove the native amorphous SiO_2 passivation layer on the surface of either the (111) or (100) Si substrates.

To make the NW arrays, a ~300 nm thick poly(methyl methacrylate) (PMMA) resist layer was first of all spin coated onto each seed surface. In order to provide patterned templates for subsequent NW growth, a regular triangular lattice (150 μm × 150 μm, with a lattice constant of 500 nm) of round growth windows (~120−130 nm in diameter) was then etched in the PMMA layer by e-beam lithography using a Jeol IC 848-2 e-beam system. After that, NW arrays were synthesized using a low temperature wet chemical method based on an aqueous solution having the same concentrations (4 mM) of zinc nitrate hexahydrate ($Zn(NO_3)_2 \cdot 6H_2O$) and hexamethylene tetramine ($(CH_2)_6N_4$), as reported elsewhere.[24] Growth time was 3 h, and the temperature was held at 85 °C. The specimens were mounted upside-down on a polytetrafluoroethylene sample holder in order to prevent any precipitates that formed in the nutrient solution from falling onto the substrates (which would have inhibited the growth of the NWs). After overnight cooling, the PMMA layer was removed in acetone and the specimens were thoroughly rinsed with deionized water. The resulting ZnO NW arrays were imaged using a Zeiss 1540XB field emission scanning electron microscope (SEM).

Before nanostructure growth, the surface of the substrates was studied by atomic force microscopy (AFM) in semicontact mode (AIST-NT, SmartSPM 1010). The thickness of the layers was determined by means of spectroscopic ellipsometry (Woollam M2000D rotating-compensator ellipsometer). The resistivity of the seed layers was measured using a four point probe method.

The crystal structure of the seed layers and NW arrays was investigated using high resolution X-ray diffraction (XRD, Bruker AXS, D8 Discover with GADDS) with a 50 μm diameter spot size, i.e. sufficiently smaller than the patterned areas. A section of the Debye−Scherrer ring was studied using a 2D-detector system. In this approach, a $2\theta/\chi$ mapping around the (0002) peak is acquired simultaneously. The dispersion in the crystallographic alignment can then be estimated from the full width at half maximum (fwhm) along the χ direction while the distribution of the c lattice parameter (and, hence, strain information) can be deduced from the fwhm along the 2θ direction.[25]

RESULTS AND DISCUSSION

The SEM images in Figure 1a−j show that while all the growths gave regular arrays with NW ~2 μm long and 110−150 nm diameter, the various seed surfaces resulted in different NW morphologies and orientations. The NWs grown on the BULK (Figure 1a and f), PLD/sapphire (Figure 1b and g), and PLD/Si (Figure 1c and h) seed surfaces were strongly aligned with the normal to the surface, while those grown on PLD/Pt/sapphire (Figure 1d and i) and Sputt/Si (Figure 1e and j) had greater dispersion in their orientation and a more tapering geometry. Moreover, the NWs grown on the BULK and PLD/sapphire showed a common relative orientation of their hexagonal crystal facets in the surface plane (Figure 1a and b). Closer observation of the NW grown on the Sputt/Si (Figure 1e and j), PLD/Pt/sapphire (Figure 1d and i), and PLD/Si (Figure 1c and h) also revealed that, in some cases, multiple NWs grew in single growth windows.

Table 1 shows the thickness, resistivity, and root mean square (rms) roughness for the different seed surfaces.

Table 1. Details of the Compared Seed Structures[a]

	seed layer				
sample	deposition	thickness (nm)	resistivity (Ω cm)	roughness (nm)	crystal structure
BULK			1.5×10^{2}	0.13	single crystal
PLD/sapphire	PLD	139	5.40×10^{-1}	0.19	epitaxial
PLD/Si	PLD	427	4.19×10^{-1}	0.98	highly textured
PLD/Pt/sapphire	PLD	218	5.12×10^{-5}	1.31	highly textured
Sputt/Si	sputtering	155	4.14×10^{-3}	1.66	textured

[a] In the case of PLD/Pt/sapphire, an effective resistivity is calculated for the ZnO/Pt bilayer.

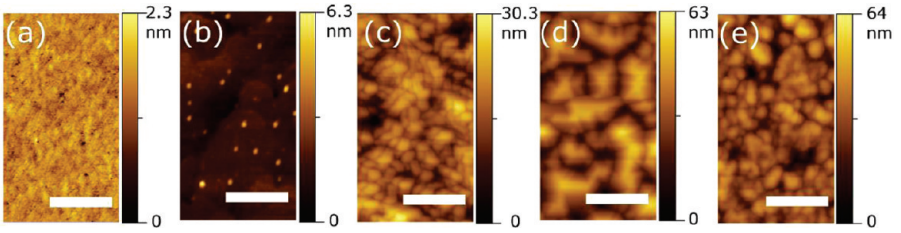

Figure 2. AFM images of ZnO seed surfaces (the length of the white scale bar is 300 nm): ZnO single crystal (a); PLD deposited ZnO on c-Al_2O_3(0001) (b); PLD deposited ZnO on Si(111) (c); PLD deposited ZnO on Pt/c-Al_2O_3(0001) (d); reactive magnetron sputtered ZnO on Si(100) (e).

The AFM images in Figure 2 suggest that the PLD/Si (Figure 2c), PLD/Pt/sapphire (Figure 2d), and Sputt/Si (Figure 2e) seed layers are composed of many tiny crystals. In the case of PLD/Si and Sputt/Si, the grains appear to range from several tens of nanometers up to hundred nanometers in diameter, while, in the case of PLD/Pt/sapphire, the grain diameters appear to be in the several hundreds of nanometer range. This could explain the presence of multiple NWs on the PLD/Si, PLD/Pt/sapphire, and Sputt/Si seed layers, since the average grain size is comparable to or lower than the diameter of the e-beam lithography patterned growth windows (~120−130 nm). Thus, there is a significant probability that more than one grain in the seed layer can nucleate in a single growth window. This explanation is supported by the observation that fewer multiple NW grew on the PLD/Pt/sapphire, which had larger crystals (Figure 2d), than the PLD/Si and Sputt/Si. The other two substrates (BULK and PLD/sapphire) have much smoother surfaces, which is consistent with significantly larger grain sizes. This could explain the common relative orientation of the NW hexagonal crystal facets as the result of epitaxial growth of the NWs on grains large enough to include many growth windows.

By comparing the rms values listed in Table 1 and the SEM images of the grown NW arrays (Figure 1), it can be seen that smoother seed surfaces have more aligned NWs. However, it is not obvious whether the roughness or the crystal structure of the seed layers is responsible for the growth direction of the NWs.

In order to establish a better understanding of the relationship between the seed layer and the NWs, a more sophisticated structural investigation was needed. Since the size of the e-beam lithography patterned areas was larger (150 μm × 150 μm) than the diameter of the X-ray beam spot (~50 μm), the patterned parts with NWs and the unpatterned parts without NWs could be examined separately.

In a pole figure measurement, a certain set of *hkl*- or *hkil*-planes is selected by fixing the detector (2Θ) and incident beam (Θ) angle. Hence, the scattering vector **S** is fixed in space, and diffraction will only occur if the normal of the selected *hkl*-/*hkil*-planes is parallel to the diffraction vector. Therefore, the sample has to be tilted (Ψ) and rotated (Φ) in space. Pole figures can be interpreted by considering the intersections of the normal to the selected *hkl*-/*hkil*-planes with an imaginary hemisphere, situated above the sample surface (Figure 3a). The projection of this hemisphere on a planar surface results in a pole figure, for which the intensity in each point is proportional to the number of grains in the film that have their normal to the selected *hkl*-planes pointing to the point with coordinates (Ψ,Φ) on the hemisphere.

XRD pole figures of the BULK crystal and the corresponding NW array revealed 6-fold rotational symmetry with sharp $\{10\bar{1}1\}$ peaks (not shown here), which can be explained by their wurtzite-type single crystalline nature. The XRD pole figure for the PLD/sapphire layer in Figure 3b also shows 6-fold symmetry for the $\{10\bar{1}1\}$ plus an epitaxial relationship based on a 30° in-plane twist with respect to the c-sapphire substrate (Figure 3c; ZnO $[10\bar{1}0]$|| sapphire $[11\bar{2}0]$),[26] as has been generally reported in the literature.[27,28] This epitaxy, in spite of a 18.4% in-plane lattice mismatch, can be explained as a result of the compliant nature of wurtzite ZnO.[29]

In the case of the PLD/Si, PLD/Pt/sapphire, and Sputt/Si samples, the seed layers and NWs all had rings in XRD pole figures, indicative of preferential *c*-axis orientation along the film growth direction and random crystallographic orientation in the film plane.[21] Indeed, the high adatom mobility in PLD allows the ZnO to crystallize readily even on amorphous substrates, such as the native SiO_2 passivation layer on the surface of the Si substrate.[30]

In previous XRD studies of the PLD ZnO/SiO_2/Si, Zerdali et al. found pole figures with sharp rings and deduced that the films had a fibrous texture with strong preferential orientation of the *c*-axis along the film normal and an *a*-axis which was oriented randomly in the film plane.[21] Such a structure is coherent with the SEM image in Figure 1c, which shows that the facets of the NWs are not aligned collectively, denoting random in-plane rotation of the NW grains. The same is true for the NWs on the PLD/Pt/sapphire and Sputt/Si surfaces (Figure 1d and e).

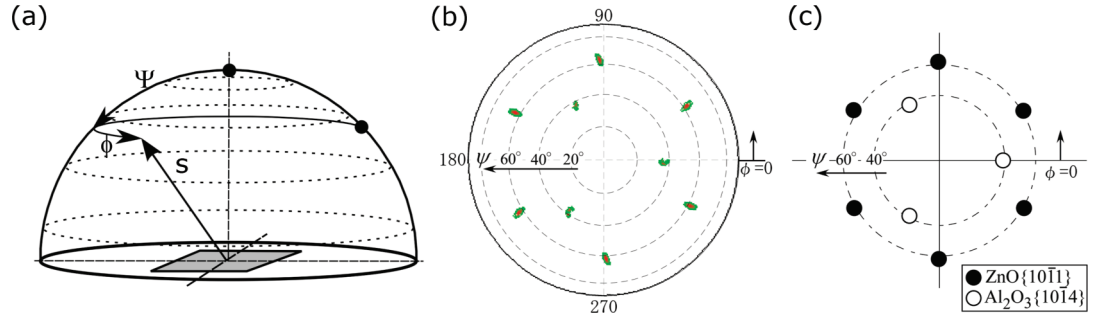

Figure 3. (a) Schematic illustration of pole figure measurement. Measured (b) and theoretical (c) pole figure for PLD deposited ZnO on c-Al_2O_3(0001).

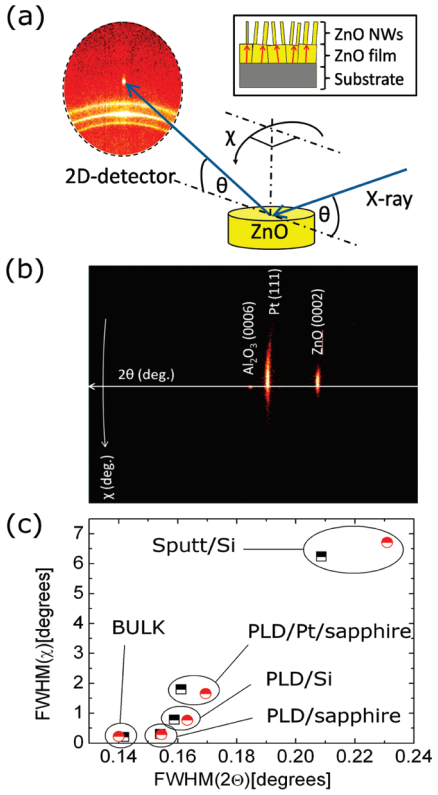

Figure 4. (a) Schematic illustration of the $2\theta-\chi$ measurement, which reveals the dispersion of the crystallographic alignment and the strain in the seed layer and in the NW array (inset). (b) Characteristic XRD pattern for PLD deposited ZnO on Pt/c-sapphire recorded by a 2D detector. (c) fwhm values of the ZnO(0002) peak along radial (2θ) and tangential (χ) paths for each seed layer (red circles) and corresponding ZnO NW arrays (black squares).

To investigate the effect of the crystal structure of the substrates on the NWs in detail, fwhm values along the χ and 2θ directions for the ZnO (0002) reflection were extracted from the XRD patterns (Figure 4a and b) and summarized in Figure 4c. The BULK and PLD/sapphire gave the lowest χ fwhm, indicating that they were the most highly oriented while the Sputt/Si was the most disordered. The χ fwhm for the NWs showed almost the same values as those for the corresponding substrates in all samples. Hence, the NW orientation appeared to reproduce the crystallographic dispersion in the seed layers.

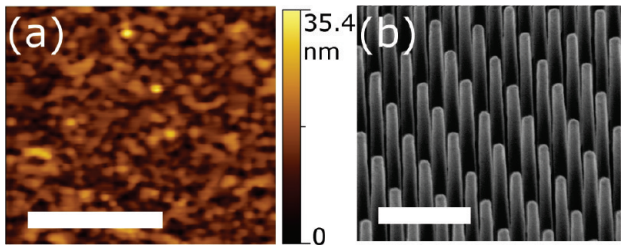

Figure 5. (a) AFM image of a PLD deposited ZnO seed layer on c-sapphire with increased roughness and (b) scanning electron micrograph for the corresponding nanowire array. The lengths of the white scale bars on the AFM and SEM images are 2 and 1 μm, respectively.

Figure 4c also shows that the 2θ fwhm for the NW arrays are significantly lower than those of their seed layer when grown on the more disoriented seed layers (Sputt/Si, PLD/Pt/sapphire, PLD/Si). This can be explained as the result of strain relaxation during NW growth.

The impact of the roughness on the NW growth was investigated by an additional PLD/sapphire type specimen having a rougher top surface. The AFM image in Figure 5a for this ZnO surface shows a significantly higher surface roughness (2.51 nm) than that for the former PLD/sapphire in Figure 2b (0.19 nm). In contrast, the SEM observations on both NW arrays show almost the same morphologies (Figures 5b and 1g). Hence, the alignment of the NWs is mainly dictated by the crystal structure of the seed surface and not by the surface roughness.

CONCLUSIONS

Regular ZnO NW arrays were grown on various ZnO seed surfaces using low temperature wet chemical growth at template windows patterned in a resist overlayer using e-beam lithography.

SEM study revealed that NW arrays which were seeded on ZnO single crystals and ZnO thin films grown epitaxially on c-sapphire by PLD showed strong *c*-axis alignment with the surface normal and a common relative orientation of their hexagonal crystal facets in the surface plane. This was taken to be indicative of *a*-axis ordering with respect to the substrate and is consistent with the NWs growing epitaxially on ZnO grains in the seed layers which were relatively large compared to the spacing of the NWs (500 nm) and thus encompassed many template windows. It can be anticipated that such in-plane ordering may offer novel properties in applications such as photonic crystals[9] or self-forming laser cavities, in which the relative orientation of

grain boundaries plays an important role, since they act as light scatterers.[31]

NW arrays grown on less oriented ZnO underlayers (on both Si and Pt/sapphire substrates) showed reduced *c*-axis alignment, and the crystallographic orientation in the plane was random. In the case of more polycrystalline ZnO seed layers, the alignment of the NWs showed increased dispersion about the normal and occasionally showed multiple NW emanating from a single nucleation window. It was inferred from AFM images that this may be due to the grain size in the seed layer being smaller than the template window in the resist layer.

Quantitative XRD and AFM analysis revealed that the crystal quality and alignment of the NWs was determined by the dispersion in the crystallographic orientation of the seed layer while the effect of the surface roughness appeared to be negligible.

The growth approach and substrate/seed-layer/NW combinations examined in this study demonstrated the potential for low-cost, wide-area fabrication of highly aligned NW arrays with precise tuning of the NW/NR dimensions and positioning plus some degree of control over the form, out-of-plane alignment, and in-plane crystallographic orientation via the choice of seed layer. This could have potential for use in applications ranging from active nanophotonic elements to energy harvesting and sensor devices.

In particular, NWs grown on epitaxial ZnO layers grown on c-sapphire by PLD gave comparable results to those grown on bulk hydrothermal substrates. This agrees with studies contrasting the homoepitaxial regrowth of ZnO thin films on hydrothermal ZnO and PLD ZnO/sapphire by chemical vapor deposition[32] and suggests that epitaxial layers on sapphire may offer a lower-cost and wider area alternative to single crystal substrates as templates for the growth of highly ordered ZnO NW arrays.

AUTHOR INFORMATION

Corresponding Author

*Telephone: +36-1-392-2222/1538. Fax: +36-1-392-2226. E-mail: volk@mfa.kfki.hu.

ACKNOWLEDGMENT

This work was supported by the Hungarian Fundamental Research Found (OTKA) under contracts PD77578 and K76287, by the János Bólyai Research Scholarship of the Hungarian Academy of Sciences as well as by the Bilateral Joint Project involving Hungary and Japan established by the Japan Society for the Promotion of Science (JSPS).

REFERENCES

(1) Chen, M.-T.; Lu, M.-P.; Wu, Y.-J.; Song, J.; Lee, Ch.-Y.; Lu, M.-Y.; Chang, Y.-Ch; Chou, L.-J.; Wang, Z. L.; Chen, L.-J. *Nano Lett.* **2010**, *10* 4387.

(2) Shen, G.; Chen, P.-C.; Ryu, K.; Zhou, C. *J. Mater. Chem.* **2009**, *19*, 828.

(3) Xu, S.; Xu, Ch.; Liu, Y.; Hu, Y.; Yang, R.; Yang, Q.; Ryou, J.-H.; Kim, H. J.; Lochner, Z.; Choi, S.; Dupuis, R.; Wang, Z. L. *Adv. Mater.* **2010**, *22*, 4749.

(4) Wang, X.; Song, J.; Liu, J.; Wang, Z. L. *Science* **2007**, *316*, 102.

(5) Choi, M.-Y.; Choi, D.; Jin, M.-J.; Kim, I.; Kim, S.-H.; Choi, J.-Y.; Lee, S. Y.; Kim, J. M.; Kim, S.-W. *Adv. Mater.* **2009**, *21*, 2185.

(6) Law, M.; Greene, L. E.; Johnson, J. C.; Saykally, R.; Yang, P. *Nat. Mater.* **2005**, *4*, 455.

(7) Qiu, J.; Li, X.; Zhuge, F.; Gan, X.; Gao, X.; He, W.; Park, S.-J.; Kim, H.-K.; Hwang, Y.-H. *Nanotechnology* **2010**, *21*, 195602.

(8) Volk, J.; Håkansson, A.; Miyazaki, H. T.; Nagata, T.; Shimizu, J.; Chikyow, T. *Appl. Phys. Lett.* **2008**, *86*, 054102.

(9) Teo, S. H. G.; Liu, A. Q.; Singh, J.; Yu, M. B.; Lo, G. Q. *Appl. Phys. A: Mater.* **2007**, *89*, 417.

(10) Wang, J. X.; Sun, X. W.; Yang, Y.; Huang, H.; Lee, Y. C.; Tan, O. K.; Vayssieres, L. *Nanotechnology* **2006**, *17*, 4995.

(11) Volk, J.; Nagata, T.; Erdélyi, R.; Bársony, I.; Tóth, A. L.; Lukács, I. E.; Czigány, Zs.; Tomimoto, H.; Shingaya, Y.; Chikyow, T. *Nanoscale Res. Lett.* **2009**, *4*, 699.

(12) Liu, R.; Vertegel, A. A.; Bohannan, E. W.; Sorenson, T. A.; Switzer, J. A. *Chem. Mater.* **2001**, *13*, 508.

(13) Huang, M. H.; Mao, S.; Feick, H.; Yan, H.; Wu, Y.; Kind, H.; Weber, E.; Russo, R.; Yang, P. *Science* **2001**, *292*, 1897.

(14) Wang, X.; Song, J.; Li, P.; Ryou, J. H.; Dupuis, R. D.; Summers, C. J.; Wang, Z. L. *J. Am. Chem. Soc.* **2005**, *127*, 7920.

(15) Wang, M.; Ye, Ch.-H.; Zhang, Y.; Wang, H.-X.; Zeng, X.-Y.; Zhang, L.-D. *J. Mater. Sci.: Mater. Electron.* **2008**, *19*, 211.

(16) Song, J.; Lim, S. *J. Phys. Chem. C* **2007**, *111*, 596.

(17) Kim, T.-U.; Kim, J.-A.; Pawar, S. M.; Moon, J.-H.; Kim, J. H. *Cryst. Growth Des.* **2010**, *10*, 4256.

(18) Kim, Y.-J.; Lee, Ch.-H.; Hong, Y. J.; Yi, G.-Ch. *Appl. Phys. Lett.* **2006**, *89*, 163128.

(19) Wei, Y.; Wu, W.; Guo, R.; Yuan, D.; Das, S.; Wang, Z. L. *Nano Lett.* **2010**, *10*, 3414.

(20) Rogers, D. J.; Teherani, F. H.; Ougazzaden, A.; Gautier, S.; Divay, L.; Lusson, A.; Durand, O.; Wyczisk, F.; Garry, G.; Monteiro, T.; Correira, M. R.; Peres, M.; Neves, A.; McGrouther, D.; Chapman, J. N.; Razeghi, M. *Appl. Phys. Lett.* **2007**, *91*, 071120.

(21) Zerdali, M.; Hamzaoui, S.; Teherani, F. H.; Rogers, D. *Mater. Lett.* **2006**, *60*, 504.

(22) Kim, T.; Yoshitake, M.; Yagyu, S.; Nemsak, S.; Nagata, T.; Chikyow, T. *Surf. Interface Anal.* **2010**, *42*, 1528.

(23) Németh, Á.; Major, Cs.; Fried, M.; Lábadi, Z.; Bársony, I. *Thin Solid Films* **2008**, *516*, 7016.

(24) Vergés, A.; Mifsud, A.; Serna, C. J. *J. Chem. Soc., Faraday Trans.* **1990**, *86*, 959.

(25) He, B. B. *Powder Diffr.* **2003**, *18*, 71.

(26) Fewster, P. F. *X-ray scattering from semiconductors*; Imperial College Press: London, 2000; Chapter 4, pp 167−276.

(27) Ohkubo, I.; Ohtomo, A.; Ohnishi, T.; Mastumoto, Y.; Koinuma, H.Kawasaki, M. *Surf. Sci.* **1999**, *443*, L1043–L1048.

(28) Steplecaru, C. S.; Martín-González, M. S.; Fernández, J. F.; Costa-Krämer, J. L. *Thin Solid Films* **2010**, *518*, 4630.

(29) Butcher, K. S. A.; Afifuddin, P.; Chen, P.-T.; Godlewski, M.; Sczerbakow, A.; Goldys, E. M.; Tansley, T. L.; Freitas, P.-T. *J. Cryst. Growth* **2002**, *246*, 237.

(30) Ougazzaden, A.; Rogers, D. J.; Teherani, F. H.; Orsal, G.; Moudakir, T.; Gautier, S.; Sandana, V. E.; Jomard, F.; Abid, M.; Molinari, M.; Troyon, M.; Voss, P. L.; McGrouther, D.; Chapman, J. N. *Proc. SPIE* **2010**, *7603*, 76031D-1.

(31) Dupont, P.-H.; Couteau, C.; Rogers, D. J.; Téhérani, F. H.; Lérondel, G. *Appl. Phys. Lett.* **2010**, *97*, 261109.

(32) Sartel, C.; Sallet, V.; Lusson, A.; Haneche, H.; Laroche, J. M.; Galtier, P.; Rogers, D. J.; Teherani, F. H. *J. Vac. Sci. Technol. B* **2009**, *27*, 1615.